factor inducing the formation of blood vessels (angiogenesis) in tumors (7). Bevacizumab is currently approved worldwide for the treatment of several types of cancer such as metastatic colorectal cancer, metastatic non-small-cell lung cancer, renal cell carcinoma, and advanced ovarian cancer, in combination with chemotherapy or interferon (8–14). Bevacizumab is also approved as a single agent for recurrent glioblastoma in the USA (15). In this context, many aspects of pathological angiogenesis have been extensively studied in many types of cancer. On the other hand, the precise role of these processes in pathogenesis of hematological malignancies including ATL is still under active investigation (16–19). Thus far, bevacizumab has not been approved for the treatment of any hematological malignancy in the USA, Europe, or Japan. The aim of the present study was to evaluate the therapeutic potential of bevacizumab with or without systemic chemotherapy for ATL and clarify the significance of angiogenesis for ATL pathogenesis, using a microenvironment-dependent murine ATL model.

Methods

Animals

NOD/Shi-*scid*, IL-2Rγ^{null} (NOG) mice (20) were purchased from the Central Institute for Experimental Animals (Kanagawa, Japan) and used at 6–8 wk of age. All of the *in vivo* experiments were performed in accordance with the United Kingdom Coordinating Committee on Cancer Research Guidelines for the Welfare of Animals in Experimental Neoplasia, Second Edition, and were approved by the Ethics Committee of the Center for Experimental Animal Science, Nagoya City University Graduate School of Medical Sciences.

Immunopathological analysis

We assessed the affected lymph nodes of 23 patients with ATL by immunopathology. The patients provided written informed consent in accordance with the Declaration of Helsinki, and this present study was approved by the institutional Ethics Committee of Nagoya City University Graduate School of Medical Sciences. Hematoxylin and eosin (HE) staining and immunostaining using anti-human CD4 (4B12; Novocastra, Wetzlar, Germany), CD25 (4C9; Novocastra), CD20 (L26; DAKO, Glostrup, Denmark), VEGF-A (sc-152, rabbit polyclonal; Santa Cruz, Heidelberg, Germany), Alpha-Smooth Muscle Actin (α-SMA) (1A4; DAKO), CD31 (JC70A; DAKO), and von Willebrand Factor (Rabbit polyclonal; DAKO) were performed on formalin-fixed, paraffin-embedded sections. VEGF-A expression levels were categorized according to the following formula: 3+ positive if ≥50%, 2+ positive if <50 ≥30%, 1+ positive if <30 ≥10%, and negative if <10% of the ATL tumor cells were stained with the corresponding antibody. Nine 100× high-power fields (HPF) of HE tumor specimens were randomly selected, and the area of tumor necrosis (%) was calculated by Image J software (21), and then averaged. Nine 100× HPF of von Willebrand Factor-stained tumor specimens were randomly selected, and numbers of vessels (per mm^2) were calculated by Image J software and then averaged.

ATL mouse model

A leukemic cell clone from a patient with ATL, which could be serially transplanted into SCID mice, designated S-YU as reported previously (22), was injected intraperitoneally (i.p.) into NOG mice. Three to 4 wk after i.p. injection, NOG mice were presented with intraperitoneal masses along the mesentery. Cells from these intraperitoneal masses were suspended in RPMI-1640 and inoculated i.p. into healthy NOG mice, which then presented with features identical to those of the original mice.

Cell lines

ATN-1, MT-1, and TL-Om1 are ATL cell lines, whereas MT-2, MT-4, and TL-Su are HTLV-1-immortalized lines, as previously described (23).

Quantitative reverse transcription-polymerase chain reaction

Total RNA was isolated with RNeasy Mini Kits (QIAGEN, Tokyo, Japan). Reverse transcription from the RNA to first strand cDNA was carried out using High Capacity RNA-to-cDNA Kits (Applied Biosystems Inc, Foster City, CA, USA). *Human VEGF-A* (Hs00900055_m1), *VEGF-R1* (Hs00176573_m1), *VEGF-R2* (Hs00911700_m1), and *β-actin* (Hs99999903_m1) *mRNA* were amplified using TaqMan® Gene Expression Assays with the aid of an Applied Biosystems StepOnePlus™. The quantitative assessment of the mRNA of interest was done by dividing its level by that of *β-actin* and expressing the result relative to Human Testis Total RNA (Clontech, Mountain View, CA, USA) as 1.0. All expressed values were averages of triplicate experiments.

Monoclonal antibodies and flow cytometry

The following Monoclonal antibodies (mAbs) were used for flow cytometry: APC-conjugated anti-human CD45 mAb (2D1; BD Biosciences, San Jose, CA, USA), PerCP-conjugated anti-CD4 mAb (SK3; BD Biosciences), PE-conjugated anti-CD25 mAb (M-A251; BD Biosciences), PE-conjugated VEGF-R1 mAb (49560; BD Biosciences), PE-conjugated VEGF-R2 mAb (89106, R&D Systems, Inc. Minneapolis, MN,

USA), and the appropriate isotype control mAbs. Whole blood was treated with BD FACS lysing solution (BD Biosciences) to remove RBC. Stained cells were analyzed on a FACSCalibur (BD Biosciences) with the aid of FlowJo software (Tree Star, Inc. Ashland, OR, USA).

Cell proliferation assay

Proliferation of S-YU and HTLV-I-immortalized lines expressing both VEGF-A and VEGF-R1 in the presence of different concentrations of bevacizumab for 48 h was assessed using CellTiter 96 Aqueous One Solution cell proliferation assay kits (Promega Corporation, Madison, WI, USA). Bevacizumab was purchased from Chugai Pharmaceutical Co., Ltd., Tokyo, Japan.

ATL cell-bearing mice treated with bevacizumab

ATL tumor cells (S-YU) from the intraperitoneal masses were suspended in RPMI-1640, and 1.0×10^7 was inoculated i.p. into each of 14 NOG mice. The animals were divided into two groups of seven each for treatment with bevacizumab or to serve as controls. Bevacizumab (10 mg/kg) or vehicle (saline) was i.p. injected into the mice 3, 10, and 17 d after tumor cell inoculations. Therapeutic efficacies were evaluated for area of tumor necrosis, number of vessels, and serum human sIL2R levels 22 d after tumor inoculation. The concentration of human sIL2R in the serum was measured by ELISA using human sIL2R immunoassay kits (R&D Systems, Inc.).

ATL cells from the intraperitoneal masses suspended in RPMI-1640 were also inoculated i.p. into another 10 NOG mice at 1.0×10^7 per mouse. These animals were randomly divided into two groups of five each for treatment with bevacizumab or as controls. Bevacizumab (10 mg/kg) or saline was injected i.p. into the mice 2, 9, 16, and 23 d after tumor cell inoculation. Therapeutic efficacy of bevacizumab was evaluated by survival times.

A further 16 NOG mice that had also received 1.0×10^7 ATL cells from intraperitoneal masses were randomly divided into two groups of eight each for treatment with bevacizumab + cyclophosphamide, doxorubicin, vincristine, prednisolone (CHOP) or CHOP alone. Bevacizumab (10 mg/kg) or saline was i.p. injected into the mice 2, 9, 16, 23, 30, and 37 d after tumor cell inoculations. CHOP was given i.p. 17 d after tumor inoculation at the following doses: cyclophosphamide, 40 mg/kg; doxorubicin, 3.3 mg/kg; vincristine, 0.5 mg/kg; and prednisolone, 0.2 mg/kg (24, 25). Therapeutic efficacy of bevacizumab was evaluated by survival time. Cyclophosphamide and vincristine were purchased from Shionogi Pharmaceutical Co., Ltd, Osaka, Japan; doxorubicin was from Kyowa Hakko Kirin Co., Ltd, Tokyo, Japan, and prednisolone was from Nippon Kayaku Co., Ltd, Tokyo, Japan.

Statistical analysis

The differences between groups regarding the tumor necrosis area, vascular number, and human sIL2R concentrations in serum were analyzed by the Mann–Whitney *U* test. In this study, $P < 0.05$ was considered significant.

Results

VEGF-A expression in ATL

VEGF-A expression by ATL cells in the lymph node lesions is shown in Fig. 1A. Immunopathological features of four cases from each group stratified by VEGF-A expression are shown in Fig. 1B. Most of the ATL cases (96%) were positive for VEGF-A.

ATL cell-bearing NOG mice

In earlier studies, S-YU ATL tumor cells, which were serially transplanted into SCID mice (22), manifested multiple enlarged mesenteric lymph nodes. In the present study, in which NOG mice rather than SCID mice were the S-YU recipients, larger tumor masses formed along the intestinal tract. Figure 2A shows the intraperitoneal masses and intestinal tract adhering tightly to one another in a NOG mouse (demarcated by thin white dotted lines in the figure). Flow cytometric analysis demonstrated that the mass mainly consisted of human cells expressing CD4 and CD25 (Fig. 2B). Immunopathological analysis revealed large atypical cells with irregular and pleomorphic nuclei, and blood vessels. The cells were CD4-positive, CD25-positive, but CD20-negative (Fig. 2C). These findings are consistent with an ATL cell phenotype in humans, and with earlier studies in the SCID/S-YU model. The S-YU tumor cells in the NOG mice were classed as VEGF-A 1+ positive (Fig. 2C). Blood vessels in the tumor tissue were stained by anti-α-SMA Ab (Fig. 2C). Vascular endothelial cells in the tumor tissue were stained by anti-von Willebrand Factor Ab, but not by anti-CD31 mAb (data not shown). Together, these results show that the blood vessels in the tumor tissue originated from the mouse, because anti-α-SMA and von Willebrand Factor Ab used in this study recognized the corresponding protein derived from both human and mouse, whereas the anti-CD31 mAb recognized the corresponding human but not murine protein (data not shown). CD4-positive CD25-positive ATL cell mild infiltration into spleen, liver, and bone marrow was seen by flow cytometry (Fig. 2D).

VEGF-A, VEGF-R1, and -R2 expression in ATL and HTLV-1-immortalized lines

VEGF-A mRNA expression was detected in all 7 ATL and HTLV-1-immortalized lines tested, and in S-YU cells

A

VEGF-A expression

Negative	Positive			
(–)	(1+)	(2+)	(3+)	
1 (4)	9 (39)	9 (39)	4 (17)	n (%)

B

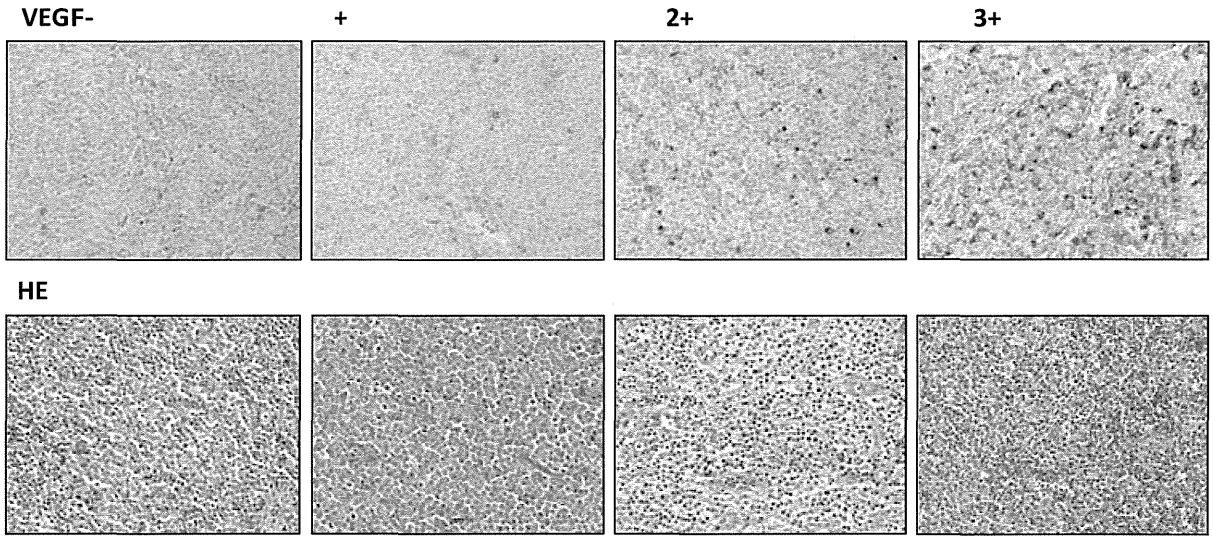

Figure 1 Vascular endothelial growth factor A (VEGF-A) expression in ATL. (A) VEGF-A expression of ATL cells in the lymph node lesion. VEGF-A expression was categorized based on the percentage of ATL cells stained as follows: ≥50%, 3+ positive; 30–49%, 2+ positive; 10–29%, 1+ positive; <10%, negative. (B) Cases 1, 2, 3, and 4 are representative of VEGF-A-negative, 1+, 2+, and 3+ positive categories, respectively. Photomicrographs with VEGF-A (upper panels) and hematoxylin and eosin staining (lower panels) are shown.

from intraperitoneal masses (Fig. 3A, upper left panel). *VEGF-R1 mRNA* expression was not present in ATL and in only two HTLV-1-immortalized lines (MT-2 and TL-Su) but was present in S-YU cells (Fig. 3A, upper right panel). No *VEGF-R2 mRNA* expression was detected in any of the 7 ATL and HTLV-1-immortalized lines tested, or in S-YU cells (data not shown). Flow cytometry demonstrated that VEGF-R1 protein was also expressed in MT-2 and TL-Su, and very weakly in NOG S-YU cells (Fig. 3A, lower panels), consistent with the RT-PCR results. Flow cytometry demonstrated that VEGF-R2 was not expressed at all in any of the ATL and HTLV-1-immortalized lines tested, or in S-YU cells (data not shown), which was also consistent with the RT-PCR results.

VEGF-R1 and VEGF-R2 expression in primary ATL cells

CD4-positive CD25-positive primary ATL cells in PBMC obtained from nine individual patients with ATL (i–ix) were evaluated for VEGF-R1 and -R2 expression. VEGF-R1 protein was expressed in only one patient (patient v) and VEGF-R2 was not expressed in any of the patients (Fig. 4B).

No Bevacizumab-mediated anti-proliferative activity against HTLV-1-immortalized lines and S-YU *in vitro*

Bevacizumab did not directly block the proliferation of MT-2 and TL-Su cells *in vitro*, despite their expression of both VEGF-A and VEGF-R1. Neither did it inhibit S-YU cells (Fig. 3C).

Therapeutic efficacy of bevacizumab monotherapy in S-YU cell-bearing NOG mice

Photomicrographs of tumor tissue from each mouse are shown (Fig. 4A). Treatment with bevacizumab resulted in an increased percentage of tumor necrosis in the NOG/S-YU mice (mean 25.3%, median 24.1%, range 19.2–33.6%), compared to control mice (mean 15.9%, median 15.4%, range 11.7–21.0%, $P = 0.0060$) (Fig. 4B, left panel). An example of calculating the percentage necrotic area is presented in Fig. 4B, right-hand panels. Bevacizumab treatment resulted in decreased vascular number in the tumor tissues [3.1, 2.6,

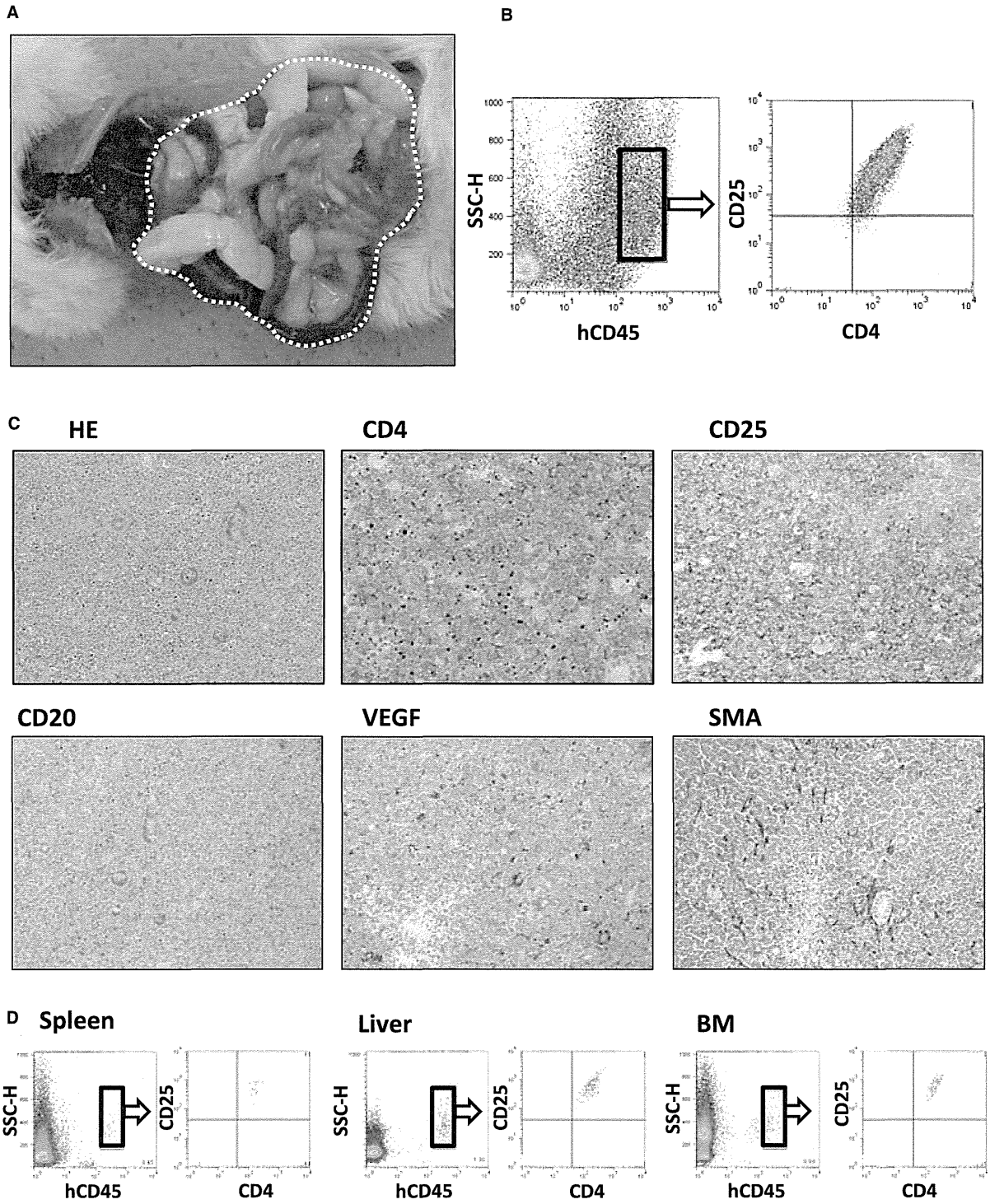

Figure 2 ATL cell-bearing NOG mouse model. (A) Macroscopic appearance of a primary DLBCL cell-bearing ATL mouse. The intraperitoneal mass is demarcated by a thin white dotted line. (B) Human CD45-positive cells in the mass determined by human CD4 and CD25 expression. (C) Immunohistochemical images of the intraperitoneal mass. (D) Human CD45-positive cells of each organ determined by human CD4 and CD25 expression.

0.0–8.3/mm^2; (mean, median, range)], compared to controls (12.8, 15.6, 1.6–19.3/mm^2, $P = 0.0127$) (Fig. 4C, left panel). An example of this calculation is presented in Fig. 4C, right-hand panels. Because sIL2R appears in the serum, concomitant with its increased expression on cells, we measured human sIL2R concentrations as a surrogate marker reflecting

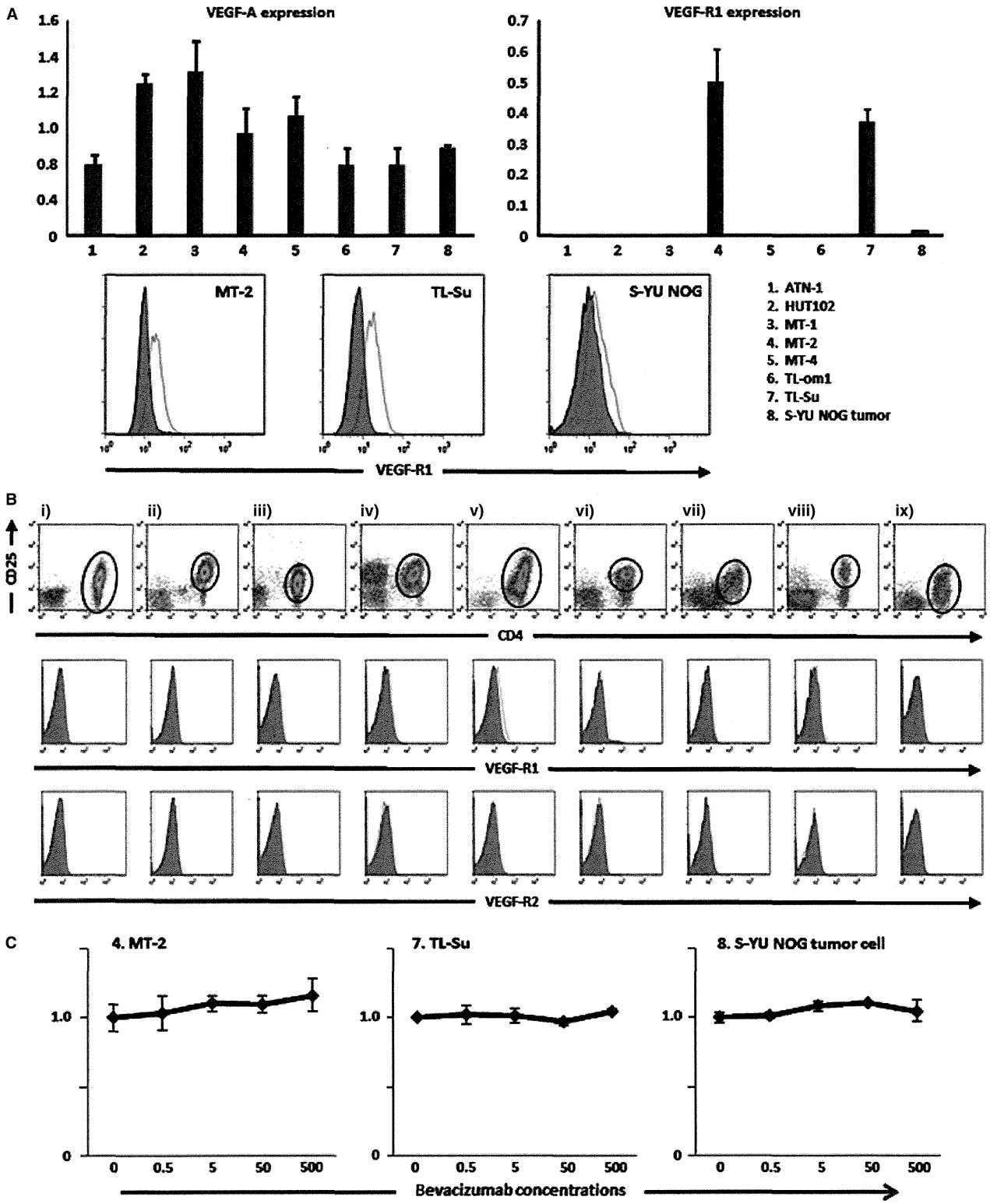

Figure 3 Vascular endothelial growth factor A (VEGF-A), VEGF-R1, and -R2 expression in primary ATL cells, or ATL and HTLV-1-immortalized lines (A) Quantitative RT-PCR analysis for VEGF-A and VEGF-R1 in 7 ATL and HTLV-1-immortalized lines, and NOG ATL cells from the intraperitoneal mass (upper panels). Flow cytometry for VEGF-R1 in HTLV-1-immortalized lines MT-2 and TL-Su, and NOG ATL cells, from the intraperitoneal mass (lower panels). (B) Flow cytometry for VEGF-R1, and -R2 in 9 primary ATL cells. (C) Bevacizumab has no direct anti-proliferative activity against HTLV-1-immortalized lines (MT-2 and TL-Su) expressing both VEGF-A and VEGF-R1, or NOG ATL cells, *in vitro*. Each result represents three independent experiments.

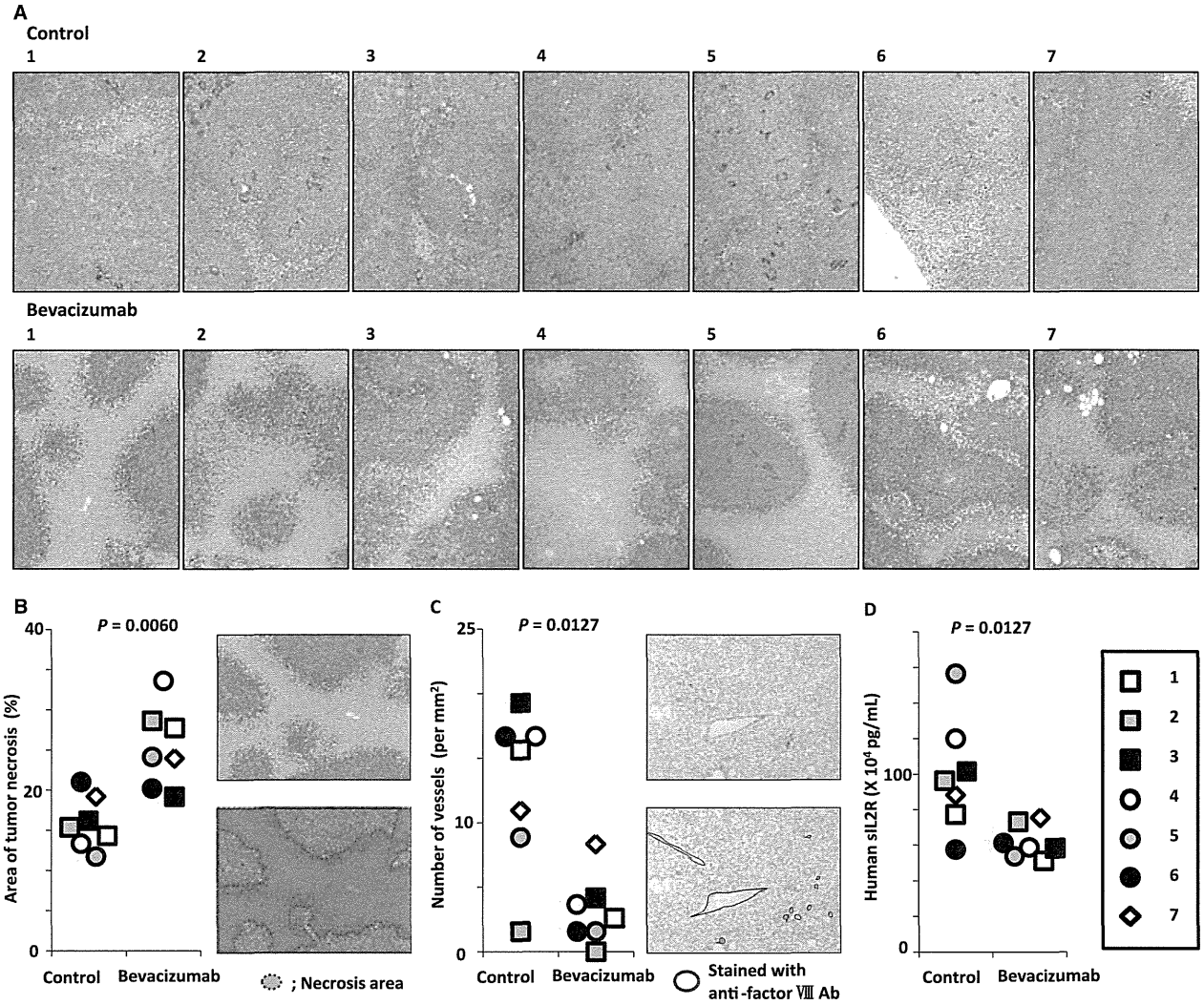

Figure 4 Bevacizumab therapy has significant therapeutic efficacy in the ATL cell-bearing NOG mouse model. (A) Macroscopic photomicrographs with hematoxylin and eosin staining of mice given saline (control) (upper panels) or bevacizumab (lower panels). (B) Area of tumor necrosis (%) of each ATL cell-bearing NOG mouse. The bevacizumab-treated mice had significantly greater tumor necrosis than control mice (left panel). An example of a calculation for tumor necrosis area (%) by means of Image J software is shown (right panels). (C) Numbers of vessels (/mm^2) of each ATL cell-bearing NOG mouse. The bevacizumab recipients had significantly fewer vessels than controls (left panel). An example of such a calculation by means of Image J software is shown (right panels). (D) Serum sIL2R concentrations of each ATL cell-bearing NOG mouse. The bevacizumab recipients had significantly lower levels of sIL2R than controls.

the tumor burden of the human CD25-expressing ATL (26). Treatment with bevacizumab showed significantly greater therapeutic efficacy as demonstrated by sIL2R concentrations in S-YU cell-bearing NOG mice (617.9, 588.5, 513.2–755.7 $\times$ 10^3 pg/mL), compared to controls (996.6, 963.4, 575.7–1565.0 $\times$ 10^3 pg/mL, P = 0.0127) (Fig. 4D). Although bevacizumab monotherapy showed significant therapeutic efficacy as demonstrated by the percentage of tumor necrosis, vascular number in the tumor tissues, and sIL2R concentrations in sera (Fig. 4), it did not confer any survival advantage to the NOG/S-YU mice (Fig. 5A). No toxicity attributable to bevacizumab injections was observed in any of the mice in this setting.

Therapeutic efficacy of bevacizumab plus CHOP compared to CHOP alone in S-YU cell-bearing NOG mice

The bevacizumab plus CHOP group did have a significant prolongation of survival compared with CHOP alone (P = 0.046). The median survival time of bevacizumab plus CHOP and CHOP alone was 38 and 34 d, respectively.

Discussion

In this study, we have demonstrated that bevacizumab possesses significant therapeutic efficacy in an ATL mouse model in which the tumor cells from a patient survive and

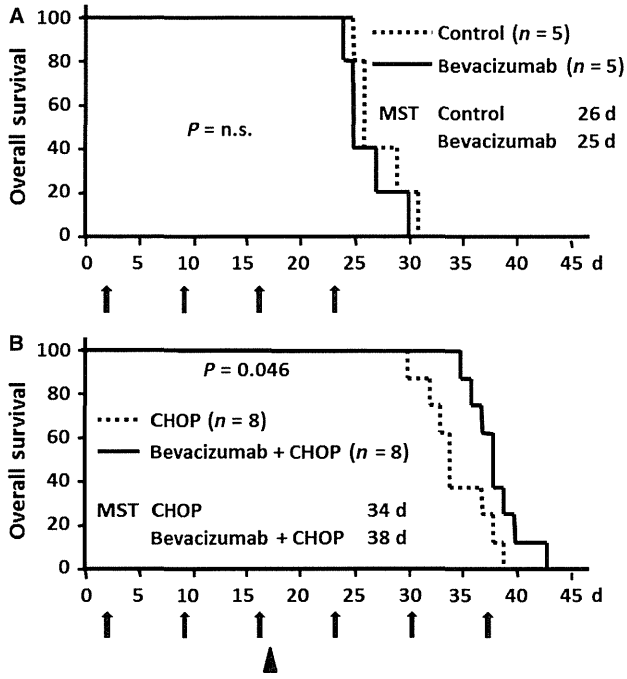

Figure 5 Survival analysis of ATL cell-bearing NOG mice treated with bevacizumab (A) Kaplan–Meier survival curves of ATL cell-bearing NOG mice treated with bevacizumab or saline. Arrows, bevacizumab or control (saline) injections. Each group consists of five mice. The difference between the bevacizumab and control groups is not significant. (B) Kaplan–Meier survival curves of ATL cell-bearing NOG mice treated with bevacizumab + CHOP, or CHOP alone. Arrows, bevacizumab or control (saline) injections. Arrow head, CHOP injection. Each group consists of eight mice. The difference between the bevacizumab + CHOP and CHOP alone is statistically significant.

proliferate in a murine microenvironment-dependent manner. The present finding revealed the importance of angiogenesis for the pathogenesis of VEGF-expressing ATL.

NOG mice have severe, multiple immune defects, such that human immune cells engrafted into them retain essentially the same functions as in humans (27, 28). While it has been reported that S-YU cells can be serially transplanted into SCID mice as recipients, the present study demonstrated that S-YU cells could also be serially transplanted into NOG mice. This was not unexpected given the even more severe immune dysfunction of NOG mice compared to SCID mice. This may also explain why the ATL tumor masses were much larger in NOG than in SCID mice.

In this study, most primary ATL cases (22/23), and all of the established cell lines tested (7/7), were positive for VEGF-A. These results are consistent with data from other investigators (16, 18, 19). Thus, the VEGF-A produced by ATL cells is likely to play an important role in the pathogenesis of ATL. On the other hand, *VEGF-R1 mRNA* expression was only seen in two of the seven ATL and HTLV-1-immortalized lines, and *VEGF–R2* in none of them. VEGF-R1 protein expression by primary ATL tumor cells was only seen in one of nine patients, and VEGF-R2 in none. In B-cell lymphomas, an earlier study reported that tumor cell growth was promoted in an autocrine fashion via VEGF-A/VEGF-R1 or VEGF-A/VEGF-R2 interactions (29). However, the present analysis of VEGF-R1/R2 expression in ATL, and the results of *in vitro* proliferation assays, did not support the existence of such an autocrine loop in ATL.

Because S-YU cells can only be maintained by serial transplantation in immunodeficient mice, but not by *in vitro* culture (30), the microenvironment is likely to be indispensable for their survival. S-YU are positive for VEGF-A, and therefore it would be expected that the interaction of VEGF-A produced by ATL cells with receptors on host (murine) endothelial cells should play an important role in tumor angiogenesis. This would lead to tumor cell survival and proliferation supported by transport of sufficient nutrients and oxygen in the mouse. Therefore, the present ATL model using S-YU should better reflect the human ATL *in vivo* environment, compared to other mouse models using established ATL cell lines, or HTLV-1-immortalized lines. Thus, this model should provide a powerful tool for understanding the pathogenesis of ATL. Furthermore, it should be useful not only for evaluating novel cytotoxic anti-ATL agents, but also provide a more appropriate *in vivo* model to test antitumor agents targeting the microenvironment, including bevacizumab.

The effect observed in mice receiving bevacizumab monotherapy, as demonstrated by the increased tumor necrosis area and reduced vasculature in the tumor tissue, was expected, given the conventional antitumor mechanism of bevacizumab, which neutralizes the human VEGF-A produced by the tumor cells, but not murine VEGF-A (31). It then inhibits the growth of new blood vessels and thus starves tumor cells of necessary nutrients and oxygen (32). This should lead to a reduced tumor burden, as indicated by the sIL2R concentrations measured. Although bevacizumab monotherapy did show this anti-angiogenesis effect, it did not lead to survival prolongation in this study. This finding is consistent with the clinical observations in many types of cancer such as colorectal cancer, non-small-cell lung cancer, renal cell carcinoma, and ovarian cancer. On the other hand, combination treatment with bevacizumab and CHOP did prolong survival compared to CHOP alone. Nonetheless, the extent of this prolongation was not marked, which is also consistent with clinical observations in many types of cancer where bevacizumab is of limited benefit and then only when combined with chemotherapy. This study suggested that the tumor cell 'starvation effect' alone mediated by bevacizumab does not result in prolonged survival. It has been reported that VEGF-targeted therapy can 'normalize' the tumor vascular network and that this can lead to a more uniform blood flow, with subsequent increased delivery of chemotherapeutic agents (33, 34). This normalization by bevacizumab is a possible explanation for the prolonged survival in the present combination setting.

The present study demonstrated the importance of angiogenesis for the pathogenesis of ATL and the potential efficacy of blocking this in at least a subgroup of patients with ATL. In recent clinical cancer therapy experience, the epidermal growth factor receptor (EGFR) tyrosine kinase inhibitor, gefitinib, failed to yield significantly improved overall survival in patients with refractory NSCLC, but did show therapeutic benefit in a subgroup of patients with mutated EGFR (35). In the case of mAb targeting the EGFR, both panitumumab and cetuximab also yield clinical benefits only in a subgroup of colorectal cancer patients with wild-type *KRAS* and BRAF (36). These findings indicate that we should develop novel treatment strategies based on tumor biology, and not on tumor category. Therefore, as a next step, further investigations are warranted to determine which subgroups of patients with ATL will benefit from bevacizumab therapy (37). In other words, we should face the challenge of developing robust biomarkers that can guide selection of those patients with ATL for whom bevacizumab therapy will be most beneficial. In addition, several promising new agents for treating ATL are currently being developed (1, 38–40). Investigations of combinations of bevacizumab with these novel agents are also warranted.

In conclusion, to the best of our knowledge this is the first report to evaluate the efficacy of bevacizumab for ATL in a tumor microenvironment-dependent animal model. Bevacizumab therapy combined with chemotherapy could be a potential treatment strategy for that subgroup of patients with ATL probably depending to a large extent on angiogenesis via VEGF for tumor survival and proliferation.

Acknowledgements

We thank Ms Chiori Fukuyama for her excellent technical assistance and Ms. Naomi Ochiai for her excellent secretarial assistance.

Funding

This study was supported by Grants-in-Aid for Scientific Research (B) (No. 25290058, T. Ishida), and Scientific Support Programs for Cancer Research (No. 221S0001, T. Ishida) from the Ministry of Education, Culture, Sports, Science and Technology of Japan, Grants-in-Aid for National Cancer Center Research and Development Fund (No. 21-6-3, T. Ishida), and H23-Third Term Comprehensive Control Research for Cancer-general-011, T. Ishida, from the Ministry of Health, Labour and Welfare, Japan.

Authorship contributions

Mori F, Ishida T, Asahi I, and Ueda R designed the research. Mori F, Ishida T, Asahi I, Sato F, Masaki A, Narita T, Suzuki S, Yamada T, and Takino H performed the research. Hishizawa M, Imada K, Takaori-Kondo A contributed to establishing the ATL mouse model. All the authors analyzed the data and wrote the article.

Conflict of interest

Nagoya City University Graduate School of Medical Sciences has received research funding for Takashi Ishida, Shigeru Kusumoto, and Shinsuke Iida from Chugai Pharmaceutical Co., Ltd. The other authors have no financial conflicts of interest related with this study.

References

1. Ishida T, Ueda R. Antibody therapy for adult T-cell leukemia-lymphoma. *Int J Hematol* 2011;**94**:443–52.
2. Matsuoka M, Jeang KT. Human T-cell leukaemia virus type 1 (HTLV-1) infectivity and cellular transformation. *Nat Rev Cancer* 2007;**7**:270–80.
3. Shimoyama M. Diagnostic criteria and classification of clinical subtypes of adult T-cell leukaemia-lymphoma. A report from the Lymphoma Study Group (1984–87). *Br J Haematol* 1991;**79**:428–37.
4. Uchiyama T, Yodoi J, Sagawa K, Takatsuki K, Uchino H. Adult T-cell leukemia: clinical and hematologic features of 16 cases. *Blood* 1977;**50**:481–92.
5. Ishida T, Hishizawa M, Kato K, *et al.* Allogeneic hematopoietic stem cell transplantation for adult T-cell leukemia-lymphoma with special emphasis on preconditioning regimen: a nationwide retrospective study. *Blood* 2012;**120**:1734–41.
6. Utsunomiya A, Miyazaki Y, Takatsuka Y, *et al.* Improved outcome of adult T cell leukemia/lymphoma with allogeneic hematopoietic stem cell transplantation. *Bone Marrow Transplant* 2001;**27**:15–20.
7. Carmeliet P, Jain RK. Molecular mechanisms and clinical applications of angiogenesis. *Nature* 2011;**473**:298–307.
8. Burger RA, Brady MF, Bookman MA, *et al.* Incorporation of bevacizumab in the primary treatment of ovarian cancer. *N Engl J Med* 2011;**365**:2473–83.
9. Escudier B, Pluzanska A, Koralewski P, *et al.* Bevacizumab plus interferon alfa-2a for treatment of metastatic renal cell carcinoma: a randomised, double-blind phase III trial. *Lancet* 2007;**370**:2103–11.
10. Escudier B, Bellmunt J, Négrier S, Bajetta E, Melichar B, Bracarda S, Ravaud A, Golding S, Jethwa S, Sneller V. Phase III trial of bevacizumab plus interferon alfa-2a in patients with metastatic renal cell carcinoma (AVOREN): final analysis of overall survival. *J Clin Oncol* 2010;**28**:2144–50.
11. Hurwitz H, Fehrenbacher L, Novotny W, *et al.* Bevacizumab plus irinotecan, fluorouracil, and leucovorin for metastatic colorectal cancer. *N Engl J Med* 2004;**350**:2335–42.
12. Perren TJ, Swart AM, Pfisterer J, *et al.* A phase 3 trial of bevacizumab in ovarian cancer. *N Engl J Med* 2011;**365**:2484–96.

13. Sandler A, Gray R, Perry MC, Brahmer J, Schiller JH, Dowlati A, Lilenbaum R, Johnson DH. Paclitaxel-carboplatin alone or with bevacizumab for non-small-cell lung cancer. *N Engl J Med* 2006;**355**:2542–50.
14. Yang JC, Haworth L, Sherry RM, Hwu P, Schwartzentruber DJ, Topalian SL, Steinberg SM, Chen HX, Rosenberg SA. A randomized trial of bevacizumab, an anti-vascular endothelial growth factor antibody, for metastatic renal cancer. *N Engl J Med* 2003;**349**:427–34.
15. Kreisl TN, Kim L, Moore K, *et al.* Phase II trial of single-agent bevacizumab followed by bevacizumab plus irinotecan at tumor progression in recurrent glioblastoma. *J Clin Oncol* 2009;**27**:740–5.
16. Bazarbachi A, Abou Merhi R, Gessain A, *et al.* Human T-cell lymphotropic virus type I-infected cells extravasate through the endothelial barrier by a local angiogenesis-like mechanism. *Cancer Res* 2004;**64**:2039–46.
17. El-Sabban ME, Merhi RA, Haidar HA, Arnulf B, Khoury H, Basbous J, Nijmeh J, de Thé H, Hermine O, Bazarbachi A. Human T-cell lymphotropic virus type 1-transformed cells induce angiogenesis and establish functional gap junctions with endothelial cells. *Blood* 2002;**99**:3383–9.
18. Hayashibara T, Yamada Y, Miyanishi T, Mori H, Joh T, Maeda T, Mori N, Maita T, Kamihira S, Tomonaga M. Vascular endothelial growth factor and cellular chemotaxis: a possible autocrine pathway in adult T-cell leukemia cell invasion. *Clin Cancer Res* 2001;**7**:2719–26.
19. Watters KM, Dean J, Gautier V, Hall WW, Sheehy N. Tax 1-independent induction of vascular endothelial growth factor in adult T-cell leukemia caused by human T-cell leukemia virus type 1. *J Virol* 2010;**84**:5222–8.
20. Ito M, Kobayashi K, Nakahata T. NOD/Shi-scid IL2rgnull (NOG) mice more appropriate for humanized mouse models. *Curr Top Microbiol Immunol* 2008;**324**:53–76.
21. Abramoff MD, Magelhaes PJ, Ram SJ. Image Processing with ImageJ. *Biophotonics Int* 2004;**11**:36–42.
22. Imada K, Takaori-Kondo A, Sawada H, Imura A, Kawamata S, Okuma M, Uchiyama T. Serial transplantation of adult T cell leukemia cells into severe combined immunodeficient mice. *Jpn J Cancer Res* 1996;**87**:887–92.
23. Suzuki S, Masaki A, Ishida T, *et al.* Tax is a potential molecular target for immunotherapy of adult T-cell leukemia/lymphoma. *Cancer Sci* 2012;**103**:1764–73.
24. Mori F, Ishida T, Ito A, *et al.* Potent antitumor effects of bevacizumab in a microenvironment-dependent human lymphoma mouse model. *Blood Cancer J* 2012;**2**:e67.
25. Mohammad RM, Wall NR, Dutcher JA, Al-Katib AM. The addition of bryostatin 1 to cyclophosphamide, doxorubicin, vincristine, and prednisone (CHOP) chemotherapy improves response in a CHOP-resistant human diffuse large cell lymphoma xenograft model. *Clin Cancer Res* 2000;**6**:4950–6.
26. Motoi T, Uchiyama T, Uchino H, Ueda R, Araki K. Serum soluble interleukin-2 receptor levels in patients with adult T-cell leukemia and human T-cell leukemia/lymphoma virus type-I seropositive healthy carriers. *Jpn J Cancer Res* 1988;**79**:593–9.
27. Ito A, Ishida T, Utsunomiya A, *et al.* Defucosylated anti-CCR4 monoclonal antibody exerts potent ADCC against primary ATLL cells mediated by autologous human immune cells in NOD/Shi-scid, IL-2R gamma(null) mice *in vivo*. *J Immunol* 2009;**183**:4782–91.
28. Masaki A, Ishida T, Suzuki S, *et al.* Autologous Tax-Specific CTL therapy in a primary adult T cell leukemia/lymphoma cell-bearing NOD/Shi-scid, IL-2Rγnull mouse model. *J Immunol* 2013;**191**:135–44.
29. Wang ES, Teruya-Feldstein J, Wu Y, Zhu Z, Hicklin DJ, Moore MA. Targeting autocrine and paracrine VEGF receptor pathways inhibits human lymphoma xenografts *in vivo*. *Blood* 2004;**104**:2893–902.
30. Koga H, Imada K, Ueda M, Hishizawa M, Uchiyama T. Identification of differentially expressed molecules in adult T-cell leukemia cells proliferating *in vivo*. *Cancer Sci* 2004;**95**:411–7.
31. Yu L, Wu X, Cheng Z, Lee CV, LeCouter J, Campa C, Fuh G, Lowman H, Ferrara N. Interaction between bevacizumab and murine VEGF-A: a reassessment. *Invest Ophthalmol Vis Sci* 2008;**49**:522–7.
32. Ellis LM, Hicklin DJ. VEGF-targeted therapy: mechanisms of anti-tumour activity. *Nat Rev Cancer* 2008;**8**:579–91.
33. Carmeliet P, Jain RK. Principles and mechanisms of vessel normalization for cancer and other angiogenic diseases. *Nat Rev Drug Discov* 2011;**10**:417–27.
34. Jain RK. Normalization of tumor vasculature: an emerging concept in antiangiogenic therapy. *Science* 2005;**307**:58–62.
35. Maemondo M, Inoue A, Kobayashi K, *et al.* Gefitinib or chemotherapy for non-small-cell lung cancer with mutated EGFR. *N Engl J Med* 2010;**362**:2380–8.
36. Bardelli A, Siena S. Molecular mechanisms of resistance to cetuximab and panitumumab in colorectal cancer. *J Clin Oncol* 2010;**28**:1254–61.
37. Lambrechts D, Lenz HJ, de Haas S, Carmeliet P, Scherer SJ. Markers of response for the antiangiogenic agent bevacizumab. *J Clin Oncol* 2013;**31**:1219–30.
38. Ishida T, Joh T, Uike N, *et al.* Defucosylated anti-CCR4 monoclonal antibody (KW-0761) for relapsed adult T-cell leukemia-lymphoma: a multicenter phase II study. *J Clin Oncol* 2012;**30**:837–42.
39. Tanosaki R, Tobinai K. Adult T-cell leukemia-lymphoma: current treatment strategies and novel immunological approaches. *Expert Rev Hematol* 2010;**3**:743–53.
40. Marçais A, Suarez F, Sibon D, Frenzel L, Hermine O, Bazarbachi A. Therapeutic options for adult T-cell leukemia/lymphoma. *Curr Oncol Rep* 2013;**15**:457–64.

IJC
International Journal of Cancer

Over one-third of African-American MGUS and multiple myeloma patients are carriers of hyperphosphorylated paratarg-7, an autosomal dominantly inherited risk factor for MGUS/MM

Carsten Zwick[1], Gerhard Held[1], Michaela Auth[1], Leon Bernal-Mizrachi[2], John D. Roback[3], Susan Sunay[3], Shinsuke Iida[4], Yoshiaki Kuroda[5], Akira Sakai[6], Marita Ziepert[7], Ryuzo Ueda[8], Michael Pfreundschuh[1]* and Klaus-Dieter Preuss[1]*

[1] Department of Internal Medicine I, José-Carreras-Center for Immuno and Gene Therapy, Homburg/Saar, Germany
[2] Department of Hematology and Medical Oncology, Winship Cancer Institute, Emory University School of Medicine, Atlanta, GA
[3] Department of Pathology and Laboratory Medicine, Emory University School of Medicine, Atlanta, GA
[4] Department of Medical Oncology and Immunology, Nagoya City University, Nagoya, Japan
[5] Department of Hematology and Oncology, Division of Clinical Research, Research Institute for Radiation Biology and Medicine, Hiroshima University, Hiroshima, Japan
[6] Department of Radiation Life Science, Fukushima Medical University, Fukushima, Japan
[7] The Institute for Medical Informatics, Statistics and Epidemiology (IMISE), Leipzig University, Leipzig, Germany
[8] Department of Tumor Immunology, Aichi Medical University, Nagakute, Japan

As hyperphosphorylated paratarg-7 (pP-7) carrier state was shown to be the first molecularly defined autosomal dominantly inherited risk factor for monoclonal gammopathy of unknown significance (MGUS) and multiple myeloma (MM) in a European population, the prevalence of pP-7 carrier state among African-Americans who have a significantly higher incidence of MGUS/MM is of interest. We therefore determined pP-7 carrier state and paraproteins with specificity for P-7 in African-American, European and Japanese patients with MGUS/MM and healthy controls. By isoelectric focusing and ELISA, a paratarg-7-specific paraprotein and the associated pP-7 carrier state was observed in 30/81 (37.0%) African-American, 42/252 (16.7%) European and 7/176 (4.0%) Japanese MGUS/MM patients ($p < 0.001$). A pP-7 carrier state was found in 11/100 (11.0%) African-American, 8/550 (1.5%) European and 1/278 (0.4%) Japanese healthy controls ($p < 0.001$), resulting in an odds ratio for MGUS/MM of 4.8 ($p < 0.001$) among African-American, 13.6 among European ($p < 0.001$) and 11.5 ($p = 0.023$) among Japanese carriers of pP-7. We conclude that pP-7 carriers are most prevalent among African-Americans, but a pP-7 carrier state is the strongest molecularly defined single risk factor for MGUS/MM known to date in all three ethnic groups. The high prevalence of pP-7 carriers among African-American patients emphasizes a predominant role of this genetic factor in the pathogenesis of these diseases. The large number of pP7 African-American patients and controls should facilitate the identification of the SNP or mutation underlying the pP-7 carrier state.

A causal relationship between monoclonal gammopathy of unknown significance (MGUS) and multiple myeloma (MM) and chronic antigenic stimulation has been suggested by the results of several studies[1]; hence, the identification of the antigenic stimuli of B-cell neoplasms is of interest. In a modification of SEREX[2] using a commercially available human fetal brain-derived protein macroarray and IgA or IgG paraprotein-containing sera, paratarg-7 was shown to be a frequent antigenic target of paraproteins from European patients with MGUS, MM and Waldenstrom's macroglobulinemia.[3–5] All patients with paratarg-7-specific paraproteins were carriers of a hyperphosphorylated version of the protein (pP-7) and this hyperphosphorylation is inherited in a dominant fashion.[3–5] The hyperphosphorylation of paratarg-7 in these patients is due to an inactivation of protein phosphatase 2A resulting in the failure to dephosphorylate the physiologically occurring phosphorylation of p-7 at serine 17.[6] Paratarg-7 is identical to STOML2 (stomatin [EPB72]-like), also known as HSPC108 or stomatin-like-protein and SLP-2,[7] which is expressed in all human tissues.[8] The physiological function of SLP-2 is unknown. As few healthy Europeans are carriers of pP-7, pP-7 carrier state is associated with an

Key words: MGUS, multiple myeloma, risk factors, genetics
*These authors contributed equally to this work
Grant sponsors: Wilhelm Sander-Stiftung (a charity organization), Deutsche Forschungsgemeinschaft (German Research Society, DFG Association), Deutsche Krebshilfe (a charity organization)
DOI: 10.1002/ijc.28731
History: Received 13 Nov 2013; Accepted 19 Dec 2013; Online 20 Jan 2014
Correspondence to: Michael Pfreundschuh, Department of Internal Medicine I, José-Carreras-Center for Immuno and Gene Therapy, Saarland University Medical School, D-66421 Homburg (Saar), Germany, Tel.: +49-6841-162-3002, Fax: +49-6841-162-3101, E-mail: michael.pfreundschuh@uks.eu

What's new?

African-Americans are more than twice as likely as the general population to develop monoclonal gammopathy of unknown significance (MGUS) and multiple myeloma (MM). A hyperphosphorylated form of the protein paratarg-7, called pP-7, is a dominantly inherited risk factor for MGUS/MM. In this study, the authors found that more than one third of African-American MGUS/MM patients expresspP-7. This suggests that pP-7 might play a role in the pathogenesis of MGUS/MM, and should facilitate the identification of the SNP or mutation responsible for the pP-7 carrier state.

increased risk for MGUS/MM. Thus, pP-7 is the first molecularly defined inherited risk factor for any hematological neoplasm known to date. The incidence of MGUS and MM is lower in Asians and higher in African-Americans than in Europeans[9,10]; therefore, we compared these three ethnic groups with respect to the prevalence of a pP-7 carrier state and the incidence of P-7-specific paraproteins in MGUS/MM and healthy controls.

Material and Methods

Patients and controls

This study was approved by the local ethical review boards of the participating institutions. Consecutive patients with MGUS/MM with an IgA, IgD or IgG paraprotein were included. Healthy European, Japanese and African-American blood donors served as controls. Healthy was defined as having no monoclonal immunoglobulin by serum electrophoresis and immunofixation, and being healthy as diagnosed by the Medical Officer in the pre-donation check-up. Samples of African-American MGUS/MM patients and patients with other malignant diseases were collected at Emory University Hospital in Atlanta, GA, as were healthy African-American controls. Autoimmune-disease blood samples were obtained from patients diagnosed and treated at the Autoimmune Disease Clinics of the Department of Internal Medicine I, Saarland University Medical School. Written informed consent was obtained from all patients and controls. Peripheral blood was centrifuged, and plasma and cells were stored at −20°C.

Isoelectric focusing for the determination of the pP-7 carrier state

The isoelectric focusing to determine the pP-7 carrier state was performed as described before.[4,6,11]

Paratarg-7 ELISA for the detection of paraproteins with specificity to paratarg-7

The paratarg-7 ELISA using full-length recombinant paratarg-7 was performed as described previously.[3]

Statistical methods

Odds ratios with 95% confidence intervals (CIs) and p-values are presented to describe the risk for MGUS/MM (in relation to healthy controls) in pP-7 carriers separately for each of the three ethnic groups. To compare the odds ratios between ethnic groups Breslow–Day tests were performed. Chi-square and if necessary Fisher's exact tests were used to test differences between ethnic groups regarding the prevalence of pP-7, separately for MM/MGUS patients and healthy controls. In case of significant global test over all three ethnic groups pairwise tests were performed. For comparison of prevalence of pP-7 carriers among healthy controls and MGUS/MM patients within each of the ethnic groups we used chi-square and if necessary Fisher's exact tests. For differences regarding patient characteristics, we calculated chi-square and if necessary Fisher's exact tests for qualitative data and Wilcoxon rank sum tests for quantitative data (Table 2). The significance level was $p = 0.05$. Statistical analyses were done with IBM SPSS Statistics 20.

Results

A total of 252 European, 176 Japanese and 81 Afro-American MGUS and MM patients were included in this study. About 30/81 (37.0%) African-American, 42/252 (16.7%) European and 7/176 (4.0%) Japanese MGUS/MM

Table 1. Detection of paratarg-7 specific paraproteins in consecutive African-American, European and Japanese patients with MGUS/MM

	MGUS (%)	MM (%)	Total (%)
African-Americans			
IgA	2/6 (33.3)	2/4 (50)	4/10 (40.0)
IgD	0/0	0/1	0/1
IgG[1]	8/22 (36.4)	18/42 (42.9)	26/64 (40.6)
Light chain	0/0	0/6	0/6
Total	10/28 (35.7)	20/53 (37.7)	30/81 (37.0)
Europeans			
IgA	1/7 (14.3)	4/24 (16.7)	5/31 (16.1)
IgD	0/0	0/0	0/0
IgG[2]	5/45 (11.1)	32/176 (18.2)	37/221 (16.7)
Total	6/52 (11.5)	36/200 (18.0)	42/252 (16.7)
Japanese			
IgA	0/4	1/32 (3.1)	1/36 (2.8)
IgD	0/0	0/11	0/11
IgG[2]	0/13	6/116 (5.2)	6/129 (4.7)
Total	0/17	7/159 (4.4)	7/176 (4.0)

[1]All pP-7 reactive IgG paraproteins were of the IgG_3 subclass except 1 IgG_1.
[2]All pP-7 reactive IgG paraproteins were of the IgG_3 subclass.

Table 2. Characteristics of African-American MGUS and MM patients who are carriers of hyperphosphorylated paratarg-7 and those who are not

	pP7$^+$ n = 30 (%)	pP7 n = 51 (%)	p-value[1]
Age (years)			
Median	64	64	0.325
Range	43–89	32–84	
Diagnosis			
MGUS	10 (33.3)	17 (33.3)	1.000
Multiple Myeloma	19 (63.3)	32 (62.7)	0.958
Stage I	3 (15.8)	3 (9.7)	0.778[2]
Stage II	7 (36.8)	11 (35.5)	
Stage III	9 (47.4)	17 (54.8)	
Unknown		1 (3.1)	
Plasmacytoma	1 (3.3)	2 (3.9)	1.000
Paraprotein			
IgG	26 (86.7)	38 (74.5)	0.194
IgG_1	1 (3.3)	23 (45.1)	<0.001
IgG_2	0 (0.0)	0 (0.0)	–
IgG_3	25 (83.3)	15 (29.4)	<0.001
IgG_4	0 (0.0)	0 (0.0)	–
IgA	4 (13.3)	6 (11.8)	1.000
IgD	0 (0.0)	1 (2.0)	1.000
Light chain	0 (0.0)	6 (11.8)	0.080
Lytic lesions			
Yes	14 (48.3)	27 (52.9)	0.688[3]
No	15 (51.7)	24 (47.1)	
Unknown		1 (3.3)	
Hemoglobin (g/dl)			
Median	11.1	11.3	0.491
Range	7.2–14.9	6.7–15.8	
Creatinine (mg/dl)			
Median	1.1	1.4	0.082
Range	0.7–5.0	0.6–20.0	
Calcium (mg/dl)			
Median	10.0	9.4	0.221
Range	2.9–13.0	7.0–14.0	
ß2 microglobulin (mg/l)			
Median	3.0	3.6	0.637
Range	2.0–31.6	1.5–19.9	
Cytogenetics			
Normal	10 (33.3)	25 (49.0)	0.169
Trisomy 3	1 (3.3)	0 (0.0)	0.370
Trisomy 8	0 (0.0)	1 (2.0)	1.000
Complex	12 (40.0)	12 (23.5)	0.117
Unknown	7 (23.3)	13 (25.5)	

[1]For qualitative data chi-square test and if necessary Fisher's exact test and for quantitative data Wilcoxon rank sum test were used.
[2]p-value for 'Stages I–III'.
[3]p-value without 'unknown'.

Table 3. Prevalence of pP-7 carrier state in African-American patients with hematological neoplasms other than MGUS/MM

Acute lymphocytic leukemia	**0/2**
Acute myeloid leukemia	0/4
Chronic lymphocytic leukemia	2/13
Chronic myeloid leukemia	2/6
Diffuse large B-cell lymphoma	2/24
Follicular lymphoma	0/7
Hodgkin lymphoma	0/8
Lymphomas, others	2/8
Total	8/72

Table 4. Prevalence of pP-7 carrier state in European patients with autoimmune diseases

Autoimmune disorder	
- Rheumatoid arthritis	1/100
- Systemic lupus erythematosus	0/30
- Polymyalgia rheumatic	0/15
- Granulomatosis with polyangiitis	0/10
- Multiple sclerosis	0/10
- Crohn's disease	0/10
- Churg–Strauss syndrome	0/5
- SAPHO syndrome	0/5
- Sjögren's syndrome	0/5
Total autoimmune disorders	1/190 (0.5%)
European healthy controls	8/550 (1.5%)

patients had a paraprotein reacting with paratarg-7. All these patients were pP-7 carriers (Table 1). Notably, the 30 African-American patients with a pP-7 specific paraprotein was the first among the total of 69 patients with an IgG paraprotein who did not belong to the IgG_3, but rather to the IgG_1 subtype. The characteristics of African-American MGUS/MM patients with p-7 specific paraproteins and with paraproteins that did not bind to paratarg-7 showed no significant differences (Table 2). The differences between ethnic groups regarding the prevalence of pP-7 among MM/MGUS patients were significant ($p < 0.001$) for the global test, as were the differences between African-American (37.0%) and European (16.7%; $p < 0.001$), African-American and Japanese (4.0%; $p < 0.001$) and European and Japanese patients ($p < 0.001$).

The prevalence of healthy pP-7 carriers was 11/100 (11.0%) among healthy African-Americans, 8/550 (1.5%) in Europeans and 1/278 (0.4%) in Japanese ($p < 0.001$ in the global test). The prevalence of pP-7 carriers in the European and Japanese controls was not different ($p = 0.286$), but the prevalence of healthy pP-7 carriers in the African-Americans were significantly higher than in the European and Japanese population ($p < 0.001$ and $p < 0.001$), respectively.

The prevalence of pP-7 carriers was lower in healthy controls than in MGUS/MM patients in all three ethnic groups (African-Americans: 11.0% vs. 37.0%, $p < 0.001$; Europeans: 1.5% vs. 16.7%, $p < 0.001$; Japanese 0.4% vs. 4.0%, $p = 0.007$) resulting in an elevated risk for MGUS/MM among healthy pP-7 carriers (odds ratio: African-Americans: 4.8 [95% CI: 2.2–10.3], $p < 0.001$; Europeans: 13.6 [95% CI: 6.3–29.3], $p < 0.001$; Japanese 11.5 [95% CI: 1.4–94.1], $p = 0.023$). Thus, pP-7 carrier state is the strongest molecularly defined single risk factor for MGUS/MM known to date in all three ethnic groups. The p-value for differences in the odds ratios for MGUS/MM among healthy pP-7 carriers was 0.058 between African-Americans and Europeans, 0.430 between African-Americans and Japanese and 0.884 between Europeans and Japanese.

Discussion

This study is the first that investigated pP-7 carrier state in African-American patients. The high prevalence of pP-7 carriers among African-American MGUS/MM patients is astonishing and intriguing. The frequency of paratarg-7 as a paraprotein target in more than one-third of all African-American MGUS/MM patients suggests a role of pP-7 in the pathogenesis of these diseases in all three ethnic groups. The fact that carriers of pP-7 are only at a higher risk for MGUS/MM and Waldenstrom's macroglobulinemia (which was not included in this study due to the very low incidence of Waldenstrom's macroglobulinemia in African-Americans), but not for other malignancies in neither the European[5] nor the African-American population (Table 3) suggests that the contribution of pP-7 to the pathogenesis is more likely to be mediated by chronic antigenic stimulation and not due to a higher intrinsic potential of cells carrying the hyperphosphorylated paratarg-7 for malignant transformation. This is also supported by the fact that while all 79 patients included in this study with a paraprotein reacting with paratarg-7 were carriers of the hyperphosphorylated version of paratarg-7, none of the 430 MGUS/MM patients with paraproteins not reacting with paratarg-7 were carriers of pP-7.

Notably, the autoimmunity in pP-7 carries appears to be specific for P-7, because we found no increased frequency of pP-7 carriers among 190 patients with autoimmune disease (Table 4).

We do not know the age of the healthy blood donors, but presumably they were considerably younger than the patients. The younger age of the donors does not affect the prevalence data, because pP-7 carriership is inherited and present from birth to death. However, some of the healthy donors might develop MGUS/MM later in their life, but this would only increase the odds ratios for MGUS/MM among healthy pP-7 carriers. We also checked the healthy carriers for anti-P-7 antibodies, because we would expect a polyclonal anti-P-7 reactivity followed by the appearance of an immortalized clone. However, so far we have not (yet) detected such a polyclonal anti-paratarg-7 reactivity in the sera of healthy pP-7 carriers.

Although the differences in the risk for MGUS/MM failed to become significant between the three ethnic groups due to the limited number of patients, there was a strong trend ($p = 0.058$) for a difference between African-Americans and Europeans, which was weaker for the smaller number of African-American and Japanese probands. The reasons for the different risk ratios to develop MGUS/MM in patients of different ethnic background remain to be determined, and might be due to either environmental or additional genetic factors. In this respect, studies of African populations from Africa or Japanese from Hawaii would be very interesting, but even though we tried hard, we got no access to such populations.

We expect the risk of a pP-7 carrier in the family of a pP-7 patient to be even considerably higher, but the number of families with multiple cases of pP-7 MGUS/MM in our database is (still) too small to prove this with a solid statistics. Nevertheless, because two robust tests are available (IEF for the identification of a pP-7 carrier state and ELISA for the detection of paraproteins with specificity for paratarg-7), the identification of family members from a pP-7 MGUS/MM patient at risk, i.e., carriers of pP-7 is an easy task.

With the frequency of pP-7 carriers among healthy African-Americans and patients with MM/MGUS, sufficient numbers of pP-7 MGUS/MM patients and healthy wtP-7 and pP-7 family members should now be available to scrutinize tumour–host interactions in the presence and absence of the antigenic pP-7 in these individuals. Most importantly, the large number of African-American pP-7 carriers both among MGUS/MM patients and healthy controls should now facilitate the dissection of the break-down of tolerance against the autoantigenic pP-7 and the identification of the SNP or mutation responsible fore the inactivation of PP2A, which causes and maintains the hyperphosphorylation of paratarg-7 in individuals with a pP-7 carrier state.[6]

Acknowledgements

The authors thank all patients and their families for participating in the study.

References

1. Greenberg AJ, Rajkumar SV, Vachon CM. Familial monoclonal gammopathy of undetermined significance and multiple myeloma: epidemiology, #risk |factors, and biological characteristics. *Blood* 2012;119: 5359–66.
2. Sahin U, Tureci O, Schmitt H, et al. Human neoplasms elicit multiple specific immune responses in the autologous host. *Proc Natl Acad Sci USA* 1995;92:11810–3.
3. Preuss KD, Pfreundschuh M, Ahlgrimm M, et al. A frequent target of paraproteins in the sera of patients with multiple myeloma and MGUS. *Int J Cancer* 2009;125:656–61.
4. Grass S, Preuss K-D, Ahlgrimm A, et al. Association of a dominantly inherited hyperphosphorylated paraprotein target with sporadic and familial multiple myeloma and monoclonal gammopathy of undetermined significance: a case-control study. *Lancet Oncol* 2009;10: 950–6.
5. Grass S, Preuss KD, Wikowicz A, et al. Hyperphosphorylated paratarg-7: a new molecularly defined risk factor for monoclonal gammopathy

of undetermined significance of the IgM type and Waldenstrom macroglobulinemia. *Blood* 2011; 117:2918–23.
6. Preuss KD, Pfreundschuh M, Fadle N, et al. Hyperphosphorylation of autoantigenic targets of paraproteins is due to inactivation of PP2A. *Blood* 2011;118:3340–6.
7. Wang Y, Morrow JS. Identification and characterization of human SLP-2, a novel homologue of stomatin (band 7.2b) present in erythrocytes and other tissues. *J Biol Chem* 2000;275: 8062–71.
8. Cui Z, Zhang L, Hua Z, et al. Stomatin-like protein 2 is overexpressed and related to cell growth in human endometrial adenocarcinoma. *Oncol Rep* 2007;17:829–33.
9. Iwanaga M, Tagawa M, Tsukasaki K, et al. Prevalence of monoclonal gammopathy of undetermined significance: study of 52,802 persons in Nagasaki City, Japan. *Mayo Clin Proc* 2007;82:1474–9.
10. Landgren O, Weiss BM. Patterns of monoclonal gammopathy of undetermined significance and multiple myeloma in various ethnic/racial groups: support for genetic factors in pathogenesis. *Leukemia* 2009;23:1691–7.
11. Grass S, Preuss KD, Thome S, et al. Paraproteins of familial MGUS/multiple myeloma target family-typical antigens: hyperphosphorylation of autoantigens is a consistent finding in familial and sporadic MGUS/MM. *Blood* 2011;118:635–7.

Aldehyde dehydrogenase^{high} gastric cancer stem cells are resistant to chemotherapy

SHIMPEI NISHIKAWA[1,2], MASAMITSU KONNO[1], ATSUSHI HAMABE[1,2], SHINICHIRO HASEGAWA[1,2], YOSHIHIRO KANO[1,2], KATSUYA OHTA[1,2], TAKAHITO FUKUSUMI[1,3], DAISUKE SAKAI[1], TOSHIHIRO KUDO[1], NAOTSUGU HARAGUCHI[2], TAROH SATOH[1], SHUJI TAKIGUCHI[2], MASAKI MORI[2], YUICHIRO DOKI[2] and HIDESHI ISHII[1]

Departments of [1]Frontier Science for Cancer and Chemotherapy, [2]Gastroenterological Surgery and [3]Otorhinolaryngology - Head and Neck Surgery, Osaka University Graduate School of Medicine, Suita, Osaka 565-0871, Japan

Received November 2, 2012; Accepted December 10, 2012

DOI: 10.3892/ijo.2013.1837

Abstract. Cancer stem cells (CSCs) are known to influence chemoresistance, survival, relapse and metastasis. Aldehyde dehydrogenase (ALDH) functions as an epithelial CSC marker. In the present study, we investigated the involvement of ALDH in gastric CSC maintenance, chemoresistance and survival. Following screening for eight candidate markers (CD13, CD26, CD44, CD90, CD117, CD133, EpCAM and ALDH), five gastric cancer cell lines were found to contain small subpopulations of high ALDH activity (ALDH^{high} cells). We also examined the involvement of ALDH^{high} cell populations in human primary tumor samples. Immunodeficient NOD/SCID mice were inoculated with tumor tissues obtained from surgical specimens. ALDH^{high} cells were found to persist in the xenotransplanted primary tumor samples. In the immunodeficient mice, ALDH^{high} cells exhibited a greater sphere-forming ability *in vitro* and tumorigenic potential *in vivo*, compared with subpopulations of low ALDH activity (ALDH^{low} cells). Cell cultures treated with 5-fluorouracil and cisplatin exhibited higher numbers of ALDH^{high} cells. *Notch1* and *Sonic hedgehog (Shh)* expression was also found to increase in ALDH^{high} cells compared with ALDH^{low} cells. Therefore, it can be concluded that ALDH generates chemoresistance in gastric cancer cells through *Notch1* and *Shh* signaling, suggesting novel treatment targets.

Correspondence to: Professor M. Mori, Department of Gastroenterological Surgery, Osaka University Graduate School of Medicine, 2-2 Yamadaoka, Suita, Osaka 565-0871, Japan
E-mail: mmori@gesurg.med.osaka-u.ac.jp

Professor Hideshi Ishii, Department of Frontier Science for Cancer and Chemotherapy, Osaka University Graduate School of Medicine, 2-2 Yamadaoka, Suita, Osaka 565-0871, Japan
E-mail: hishii@gesurg.med.osaka-u.ac.jp

Key words: gastric cancer, cancer stem cells, chemotherapy resistance, aldehyde dehydrogenase

Introduction

The discovery of cancer stem cells (CSCs) in hematopoietic malignancies (1) has revealed that tumor tissues comprise a bulk of proliferating or differentiated tumor cells derived from small populations of self-renewing cells (2). Since their identification in leukemia, CSCs have been detected in solid tumors of the head and neck (3), gastrointestinal system (4), colon (5,6), breast (7) and brain (8,9). CSCs are tumorigenic, which is evident from xenotransplantation in immunodeficient mice, and are resistant to chemoradiation, whereas daughter cells are chemoradiation-sensitive (10,11). Recent studies have demonstrated that CSCs survive chemo- and radiation therapy in hypoxic regions of tumors (10,11). Studies of cell-autonomous mechanisms have revealed the involvement of anaerobic glycolysis in CSC maintenance and chemoradiation resistance (10,11). For example, CD13/aminopeptidase N, a liver CSC marker, regulates reactive oxygen species (ROS) through recycling reduced glutathione (GSH), thus contributing to intracellular ROS decrease following chemoradiation exposure (12). Similarly, intracellular ROS are suppressed after chemoradiation therapy through the activity of the hyaluronic acid receptor, CD44, an adhesion molecule expressed in cancer stem-like cells that directly interacts with pyruvate kinase M2, which is putatively involved in anaerobic glycolysis in CSCs (13). Furthermore, the CD44 variant (CD44v) has been shown to interact with xCT, a glutamate-cystine transporter, and to control intracellular GSH levels (14). CD44 abrogation has been shown to cause a loss of xCT from the cell surface, to suppress tumor growth in a transgenic gastric cancer (GC) mouse model and stimulate the p38 (mitogen-activated protein kinase) pathway (a downstream target of ROS) and the expression of the cell cycle inhibitor, p21(CIP1/WAF1), suggesting that CD44 plays a role in GSH synthesis and protection against ROS in gastrointestinal cancers (14). Taken together, these data indicate that cancer metabolism is critical for the initiation and progression of gastrointestinal CSCs.

In the present study, we investigated cell surface markers in gastric CSCs and after screening eight candidate markers

(CD13, CD26, CD44, CD90, CD117, CD133, EpCAM and ALDH), we confirmed the involvement of aldehyde dehydrogenase (ALDH) in sphere formation, tumorigenicity and chemoresistance. Throughout the study of the ALDH pathway, a cancer metabolism regulator, we encountered stemness genes, suggesting novel molecular therapeutic targets.

Materials and methods

Cell lines and cell culture. The human GC cell lines, AGS, NUGC3, GSU, MKN1, MKN7, MKN28, MKN45 and MKN74, were cultured in RPMI-1640 medium (Sigma), supplemented with penicillin, streptomycin and 10% fetal bovine serum, in plastic culture dishes (Corning). Spheres were cultured in Gibco® Dulbecco's modified Eagle's medium with nutrient mixture F-12 (Invitrogen), supplemented with 20 ng/ml human recombinant epidermal growth factor (Promega), 20 ng/ml basic fibroblast growth factor (PeproTech Inc.), B-27® Supplement (Invitrogen) and N2 Supplement (Wako), in low-attachment dishes (Corning).

Cell staining and flow cytometry. Cultured cells were harvested and stained using an Aldefluor® stem cell detection kit (StemCell Technologies) for 45 min at 37˚C. To stain cell surface markers, cells were incubated on ice with antibodies against CD44, CD26, CD117, CD90 (all from BD Biosciences), EpCAM (BioLegend) and CD133 (Miltenyi). Isotype antibodies were used as the negative controls. Discrimination between live and dead cells was carried out using the Live/Dead® Fixable Yellow Dead Cell Stain kit (Invitrogen). Mouse cells were identified by anti-H2kd (eBioscience) and anti-mouse CD45 (eBioscience) antibodies.

Primary surgical specimens and xenografts. Tumor tissues were digested into single cells with collagenase (Roche) and DNase (Worthington) at 37˚C for 1 h. Staining for fluorescence-activated cell sorting (FACS) analysis was performed, as described above. For xenografting, cells were injected subcutaneously with Matrigel® into NOD/SCID mice. All the animal experiments were performed with approval of Animal Experiments Committee of Osaka University.

RNA extraction, cDNA synthesis and quantitative PCR. Total RNA was extracted using TRIzol® reagent. cDNA was synthesized using SuperScript® (Invitrogen). Quantitative PCR was performed using LightCycler® 480 Real-Time PCR system. All procedures were performed according to the manufacturer's instructions.

Statistical analysis. Statistical significance was determined using the Student's t-test. Analyses were performed using JMP software.

Results

Screening of CSC markers in GC cell lines. We examined novel markers in gastric CSCs, if: i) they had been previously reported in other tumor types and for which useful antibodies were available for FACS analysis; ii) they were expressed in small populations (<50%) in the cell lines; and iii) these observations were evident in more than half the cell lines.

We investigated the functions of cell surface markers and intracellular molecules (ALDH) to establish a functional detection system. We screened six GC cell lines (AGS, NUGC3, GSU, MKN7, MKN1 and MKN45) for gastric CSC markers using eight candidate markers expressed in other CSCs (CD13, CD26, CD44, CD90, CD117, CD133, EpCAM and ALDH) (11). As shown in Table I, FACS analysis revealed a high expression of EpCAM in all the cell lines (almost 100% postive cells), whereas CD90, CD117 and CD133 expression was uniformly undetectable or negative. CD26 expression was positive (>50%) in four of the cell lines, but undetectable or negative in the other two, suggesting that CD26 expression depends on individual cell lines rather than the heterogeneous conditions of cell line subpopulations. CD13 expression was detected in only one cell line, GSU. Conversely, the investigation of ALDH indicated that the proportion of cells highly expressing ALDH (ALDH^{high} cells) was relatively small (6.2-45.5%) compared with the other markers (CD13, CD26, CD90, CD117, CD133 and EpCAM; Table I and Fig. 1A). Moreover, the ALDH^{high} cell populations reproducibly disappeared upon the addition of the ALDH inhibitor, diethylaminobenzaldehyde (DEAB), indicating the specificity of detection in ALDH^{high} cell populations. Reportedly, ALDH1A1, a substrate for DEAB inhibition, has been shown to be responsible for ALDH activity in CSCs (15). Thus, we focused on ALDH activity.

Cells expressing high levels of ALDH also express CD44. We examined CD44 expression, reportedly a CSC marker in breast, colon, esophageal and gastric cancers (11,13,14). Two-dimensional analysis data indicated that ALDH^{high} cell populations represented only a small subpopulation of CD44-positive cells, suggesting that ALDH is a good candidate as a CSC marker in GC (Table 1 and Fig. 1B).

Cells expressing high ALDH exist in xenografts in immunodeficient mice. We then examined the involvement of ALDH^{high} cell populations in human primary tumor samples. Primary tumor tissues from surgical specimens were obtained with written informed consent and inoculated into immunodeficient NOD/SCID mice. Approximately 30% of inoculated primary samples formed tumors in the mice after several weeks. The probability of tumor formation is likely influenced by tumor tissue viability (nutrients, necrosis and therapy-related damage), vasculogenesis in the mice (dependent on local conditions) and CSC conditions within primary samples. The tumor sample from a patient was subjected to FACS analysis. The data indicated that 57% of the human living tumor cells (separated by FACS using the Live/Dead Fixable Yellow Dead Cell Stain system and distinguished from mouse cells using anti-H2kd and CD45 antibodies) expressed active ALDH (Fig. 1C), indicating that ALDH^{high} cells are present in primary human tumor sample.

Sphere formation and tumorigenicity of populations expressing high levels of ALDH. We then examined stemness in ALDH^{high} cells. A culture of FACS-sorted ALDH^{high} cells in serum-free medium resulted in the frequent formation of large spheres compared with cells expressing low ALDH (ALDH^{low} cells; Fig. 2A and B), suggesting that ALDH^{high} cells possess a greater self-renewal ability, a critical charac-

Table I. Screening for common CSC markers using six GC cell lines.

	ALDH	CD44	EpCAM	CD133	CD13	CD26	CD90	CD117
AGS	-	+	++	-	-	-	-	-
GSU	+	++	++	-	++	++	-	-
NUGC3	+	+	++	-	-	-	-	-
MKN1	+	++	++	-	-	++	-	-
MKN7	+	++	++	-	-	++	-	-
MKN45	+	++	++	-	-	++	-	-

-, <1%. +, <50%. ++, 50-100%.

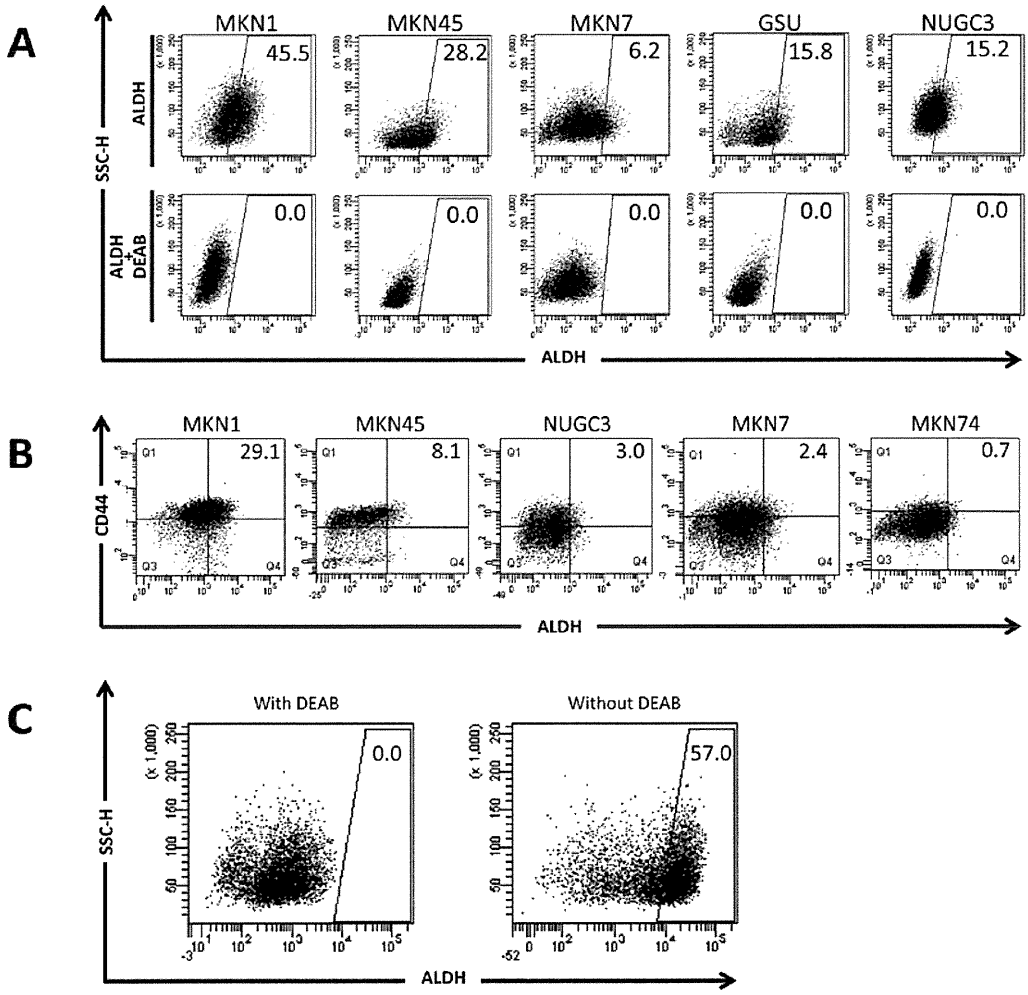

Figure 1. Aldehyde dehydrogenase (ALDH) and the other marker expression in gastric cancer cell lines. (A) ALDH in five gastric cancer (GC) cell lines. Diethylaminobenzaldehyde (DEAB) was used to inhibit ALDH activity, to show the specificity of detection. (B) Double detection of CD44 and ALDH in GC cells. $ALDH^{high}$ cells are a small fraction of $CD44^{+}$ cells. (C) Study of human primary GCs. NOD/SCID mouse xenografted tumor contains $ALDH^{high}$ cells.

teristic of CSCs (2,11). We examined tumorigenicity *in vivo* by inoculating FACS-sorted $ALDH^{high}$ and $ALDH^{low}$ MKN45 cells subcutaneously into NOD/SCID mice. We performed a limiting dilution experiment by reducing the number of inoculating cells. The inoculation of 500 $ALDH^{high}$, but not $ALDH^{low}$ cells resulted in tumor formation in three out of four mice (Fig. 2C). The inoculation of 5,000 cells resulted in tumors being formed from the $ALDH^{high}$ and $ALDH^{low}$ cells (Fig. 2C). Taken together, these observations indicate that, although multiple factors may be involved, ALDH function is closely associated with the initiation, maintenance and progression of CSCs *in vitro* and *in vivo*.

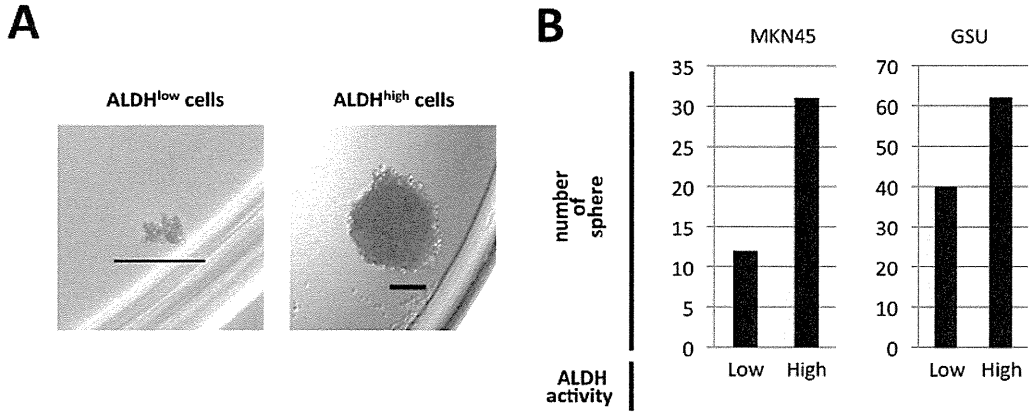

C

number of transplanted cell	ALDH^{low}	ALDH^{high}
50	0/4	0/4
500	0/4	3/4
5000	3/4	4/4

Figure 2. Sphere formation and tumorigenicity of cells expressing high and low aldehyde dehydrogenase (ALDH). (A) Representative images of sphere formation assay in MKN45 cells. After sorting ALDH^{high} and ALDH^{low} cells, they were subjected to sphere formation assay. Scale bar, 200 μm. (B) Number of spheres formed by ALDH^{high} and ALDH^{low} MKN45 and GSU cells. (C) Tumorigenicity in NOD/SCID mice. The numbers of mice that formed MKN45 tumors are shown.

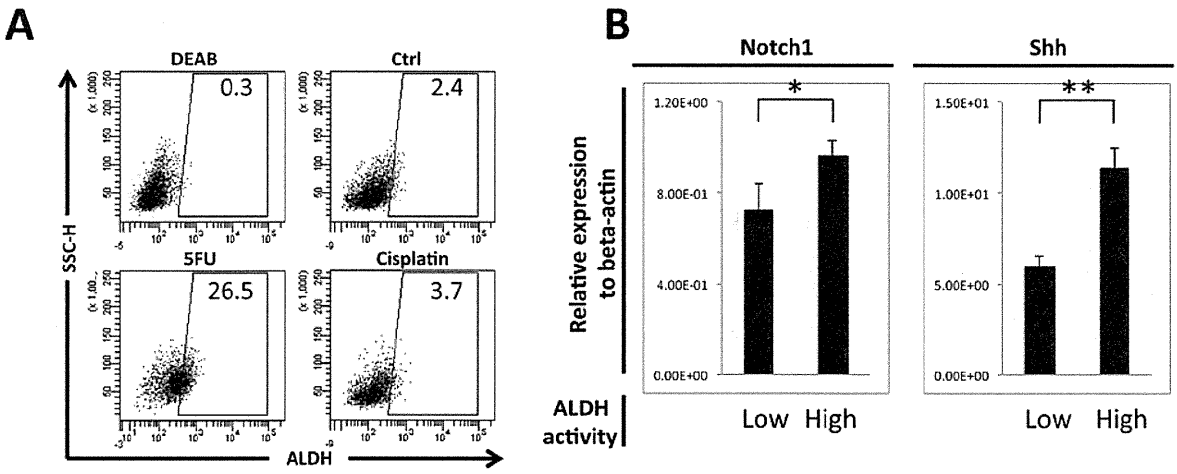

Figure 3. Chemosensitivity and the underlying mechanisms in cells showing high and low expression of aldehyde dehydrogenase (ALDH). (A) Activity of ALDH following exposure to chemotherapeutic agents. ALDH activity was assessed by fluorescence-activated cell sorting after MKN28 cells were cultured in medium containing cisplatin or 5-fluorouracil. (B) Expression of *Notch1* and *Sonic hedgehog (Shh)*. Quantitative reverse transcription PCR was used to detect the higher expression of *Notch1* and *Shh* in ALDH^{high} MKN45 cells. *P<0.05, **P<0.01.

Chemoresistance in cells highly expressing ALDH and the underlying mechanisms. Our aim was the identification of novel molecular therapeutic targets. Reportedly, CSCs can survive toxic injuries and chemoradiation therapy (2,10,11). To combat this, we explored the effect of chemotherapeutic agents commonly used to treat GC. The exposure of the cell cultures to cisplatin and 5-fluorouracil (5-FU) increased the number of ALDH^{high} cells (3.1-4.4% with cisplatin and 31.0% with 5-FU treatment; Fig. 3A), indicating that exposure to these chemotherapeutic agents causes an accumulation of surviving ALDH^{high} CSCs. To elucidate the molecular mechanisms underlying this chemoresistance, we examined gene expression changes in candidate pathways (11). We found that *Notch1* and *Sonic hedgehog (Shh)* expression was increased in ALDH^{high}, compared to ALDH^{low} cells, suggesting that the survival of ALDH^{high} cells following chemotherapy is associated with increased *Notch1* and *Shh* signaling.

Discussion

The demonstration of an association between ALDH and tumors was first shown in breast cancer (16) and subsequently in pancreatic (17), liver (18), colorectal (19), head and neck (19), thyroid (20) and lung (21) cancers. In lung cancer, ALDH activity has been shown to be selective for adenocarcinoma stem cells, depending on *Notch* signaling (21), in agreement with our observations of gastric CSCs. We demonstrated that in GC, *Notch* and *Shh* signaling may be important for both CSC maintenance and the generation of chemoresistance, providing the rationale for further study of therapy-resistant $ALDH^{high}$ CSCs. ALDH is widely used as a marker to identify and isolate various types of normal stem cells and CSCs (22). In GC, several markers reportedly characterize CSCs: CD133 (23), CD44 (23-26), side-populations identified by FACS (27), CD44 and EpCAM (25), CD54 (26) and CD90 (28). Of these markers, CD44 and ALDH are involved in aerobic glycolysis during cancer metabolism. Although an association between ALDH and the clinicopathlogical features of GC has been reported (29), the relevance of ALDH to chemoresistance has yet to be fully investigated; another study detected no association between immunohistochemical staining for ALDH and prognosis in GC patients (23). In this study, we examined for the first time the involvement of ALDH in chemoresistance and identified a candidate underlying molecular mechanism for this resistance.

GC is the second major cause of cancer-related mortality worldwide and is prevalent across Asia. *Helicobacter pylori* (*H. pylori*) infection was identified in 1982 by Marshall and Warren in patients with chronic gastritis and gastric ulcers (30). *H. pylori*-associated GC has been investigated in order to elucidate the mechanisms underlying gastric tissue damage. In general, the two mechanisms by which *H. pylori* promotes cancer are as follows: i) enhanced production of free radicals proximal to the *H. pylori* infection site, increasing the host cell mutation rate; and ii) pregenetic factors that transform host cell phenotypes by altering adhesion proteins or inflammation-related cytokines/chemokines, such as tumor necrosis factor-α or interleukin-6. Thus, *H. pylori* infection causes enhanced migration or invasion of damaged epithelial cells, without additional tumor suppressor gene mutations (31). Those non-cell autonomous mechanisms are likely facilitated by the hypoxic microenvironment of tumors, since recent studies have implicated hypoxia in inflammatory reactions provoked by *H. pylori* infection (32). Indeed, hypoxia-inducible factor-1α is mediated by the induction of a ROS-inducible protein (apurinic/apyrimidinic endonuclease 1) and its enhanced interaction with the transcriptional coactivator, p300, leads to transformed phenotypes in *H. pylori*-infected gastric epithelia (33). Although *H. pylori* infection and related atrophic gastritis are closely associated with GC, hypoxia and its related metabolism play a critical role in tumor initiation and progression in the stomach and likely in other organs (34). Further studies are warranted to elucidate the association between *H. pylori* infection and ALDH-positive CSCs in hypoxic areas and to evaluate the eradication of *H. pylori* infection and GC treatment by surgery, chemotherapy and molecular targeting of therapy-resistant CSC functions.

Acknowledgements

We thank Miyuki Ozaki and Yuko Noguchi for technical support. The current study was partly supported by a Core Research Grant-in-Aid for Scientific Research from the Ministry of Education, Culture, Sports, Science and Technology, Japan (to H.I. and M.M.); a Grant-in-Aid from the Third Term Comprehensive 10-year Strategy for Cancer Control of the Ministry of Health, Labour and Welfare, Japan (to H.I. and M.M.); a grant from the Kobayashi Cancer Research Foundation (to H.I.); a grant from the Princess Takamatsu Cancer Research Fund, Japan (to H.I.); and a grant from the SENSHIN Medical Research Foundation (to H.I.).

References

1. Bonnet D and Dick JE: Human acute leukemia is organized as a hierarchy that originates from a primitive hematopoietic cell. Nat Med 3: 730-737, 1997.
2. Reya T, Morrison SJ, Clarke MF and Weissman IL: Stem cells, cancer and cancer stem cells. Nature 414: 105-111, 2001.
3. Prince ME, Sivanandan R, Kaczorowski A, *et al*: Identification of a subpopulation of cells with cancer stem cell properties in head and neck squamous cell carcinoma. Proc Natl Acad Sci USA 104: 973-978, 2007.
4. Haraguchi N, Utsunomiya T, Inoue H, Tanaka F, Mimori K, Barnard GF and Mori M: Characterization of a side population of cancer cells from human gastrointestinal system. Stem Cell 24: 506-513, 2006.
5. Ricci-Vitiani L, Lombardi DG, Pilozzi E, Biffoni M, Todaro M, Peschle C and De Maria R: Identification and expansion of human colon-cancer-initiating cells. Nature 445: 111-115, 2007.
6. O'Brien CA, Pollett A, Gallinger S and Dick JE: A human colon cancer cell capable of initiating tumour growth in immunodeficient mice. Nature 445: 106-110, 2007.
7. Al-Hajj M, Wicha MS, Benito-Hernandez A, Morrison SJ and Clarke MF: Prospective identification of tumorigenic breast cancer cells. Proc Natl Acad Sci USA 100: 3983-3988, 2003.
8. Piccirillo SG, Reynolds BA, Zanetti N, *et al*: Bone morphogenetic proteins inhibit the tumorigenic potential of human brain tumour-initiating cells. Nature 444: 761-765, 2006.
9. Bao S, Wu Q, McLendon RE, *et al*: Glioma stem cells promote radioresistance by preferential activation of the DNA damage response. Nature 444: 756-760, 2006.
10. Ishii H, Iwatsuki M, Ieta K, Ohta D, Haraguchi N, Mimori K and Mori M: Cancer stem cells and chemoradiation resistance. Cancer Sci 99: 1871-1877, 2008.
11. Dewi DL, Ishii H, Kano Y, *et al*: Cancer stem cell theory in gastrointestinal malignancies: recent progress and upcoming challenges. J Gastroenterol 46: 1145-1157, 2011.
12. Haraguchi N, Ishii H, Mimori K, *et al*: CD13 is a therapeutic target in human liver cancer stem cells. J Clin Invest 120: 3326-3339, 2010.
13. Tamada M, Nagano O, Tateyama S, *et al*: Modulation of glucose metabolism by CD44 contributes to antioxidant status and drug resistance in cancer cells. Cancer Res 72: 1438-1448, 2012.
14. Ishimoto T, Nagano O, Yae T, *et al*: CD44 variant regulates redox status in cancer cells by stabilizing the xCT subunit of system xc(-) and thereby promotes tumor growth. Cancer Cell 19: 387-400, 2011.
15. Marcato P, Dean CA, Giacomantonio CA and Lee PW: Aldehyde dehydrogenase: its role as a cancer stem cell marker comes down to the specific isoform. Cell Cycle 10: 1378-1384, 2011.
16. Ginestier C, Hur MH, Charafe-Jauffret E, *et al*: ALDH1 is a marker of normal and malignant human mammary stem cells and a predictor of poor clinical outcome. Cell Stem Cell 1: 555-567, 2007.
17. Feldmann G, Dhara S, Fendrich V, *et al*: Blockade of hedgehog signaling inhibits pancreatic cancer invasion and metastases: a new paradigm for combination therapy in solid cancers. Cancer Res 67: 2187-2196, 2007.

18. Ma S, Chan KW, Lee TK, Tang KH, Wo JY, Zheng BJ and Guan XY: Aldehyde dehydrogenase discriminates the CD133 liver cancer stem cell populations. Mol Cancer Res 6: 1146-1153, 2008.
19. Huang EH, Hynes MJ, Zhang T, *et al*: Aldehyde dehydrogenase 1 is a marker for normal and malignant human colonic stem cells (SC) and tracks SC overpopulation during colon tumorigenesis. Cancer Res 69: 3382-3389, 2009.
20. Todaro M, Iovino F, Eterno V, *et al*: Tumorigenic and metastatic activity of human thyroid cancer stem cells. Cancer Res 70: 8874-8885, 2010.
21. Sullivan JP, Spinola M, Dodge M, *et al*: Aldehyde dehydrogenase activity selects for lung adenocarcinoma stem cells dependent on notch signaling. Cancer Res 70: 9937-9948, 2010.
22. Ma I and Allan AL: The role of human aldehyde dehydrogenase in normal and cancer stem cells. Stem Cell Rev 7: 292-306, 2011.
23. Wakamatsu Y, Sakamoto N, Oo HZ, *et al*: Expression of cancer stem cell markers ALDH1, CD44 and CD133 in primary tumor and lymph node metastasis of gastric cancer. Pathol Int 62: 112-119, 2012.
24. Takaishi S, Okumura T, Tu S, *et al*: Identification of gastric cancer stem cells using the cell surface marker CD44. Stem Cell 27: 1006-1020, 2009.
25. Han ME, Jeon TY, Hwang SH, *et al*: Cancer spheres from gastric cancer patients provide an ideal model system for cancer stem cell research. Cell Mol Life Sci 68: 3589-3605, 2011.
26. Chen T, Yang K, Yu J, *et al*: Identification and expansion of cancer stem cells in tumor tissues and peripheral blood derived from gastric adenocarcinoma patients. Cell Res 22: 248-258, 2012.
27. Fukuda K, Saikawa Y, Ohashi M, *et al*: Tumor initiating potential of side population cells in human gastric cancer. Int J Oncol 34: 1201-1207, 2009.
28. Jiang J, Zhang Y, Chuai S, *et al*: Trastuzumab (herceptin) targets gastric cancer stem cells characterized by CD90 phenotype. Oncogene 31: 671-682, 2012.
29. Katsuno Y, Ehata S, Yashiro M, Yanagihara K, Hirakawa K and Miyazono K: Coordinated expression of REG4 and aldehyde dehydrogenase 1 regulating tumourigenic capacity of diffuse-type gastric carcinoma-initiating cells is inhibited by TGF-β. J Pathol 228: 391-404 2012.
30. Marshall BJ and Warren JR: Unidentified curved bacilli in the stomach of patients with gastritis and peptic ulceration. Lancet 16: 1311-1315, 1984.
31. Suganuma M, Yamaguchi K, Ono Y, *et al*: TNF-alpha-inducing protein, a carcinogenic factor secreted from *H. pylori*, enters gastric cancer cells. Int J Cancer 123: 117-122, 2008.
32. Sinkovics JG: Molecular biology of oncogenic inflammatory processes. I. Non-oncogenic and oncogenic pathogens, intrinsic inflammatory reactions without pathogens and microRNA/DNA interactions (Review). Int J Oncol 40: 305-349, 2012.
33. Bhattacharyya A, Chattopadhyay R, Hall EH, Mebrahtu ST, Ernst PB and Crowe SE: Mechanism of hypoxia-inducible factor 1 alpha-mediated Mcl1 regulation in *Helicobacter pylori*-infected human gastric epithelium. Am J Physiol Gastrointest Liver Physiol 299: G1177-G1186, 2010.
34. Barker HE, Cox TR and Erler JT: The rationale for targeting the LOX family in cancer. Nat Rev Cancer 12: 540-552, 2012.